sustainability

MDPI

Article

Research on the Impact of Urban Rail Transit Network Topology on Transfer Convenience: Evidence from 50 Cities Worldwide

Qing Li [1], Zhenjun Zhu [1,*], Yunpeng Zhao [2], Xuhui Zhang [3], Xinyu Hu [1] and Wenzhe Xiong [1]

[1] College of Automobile and Traffic Engineering, Nanjing Forestry University, Nanjing 210037, China; liqing08@njfu.edu.cn (Q.L.); xinyuhu@njfu.edu.cn (X.H.); 13977189427@163.com (W.X.)
[2] Qingdao Train Depot of China Railway Jinan Bureau Group Co., Ltd., Qingdao 266000, China; yunpengzhao@njfu.edu.cn
[3] Nanjing Metro Group Co., Ltd., Nanjing 210008, China; ttlvescie@gmail.com
* Correspondence: zhuzhenjun@njfu.edu.cn

Abstract

Previous research on urban rail transit (URT) transfer convenience mainly focused on the transfer stations, often neglecting the impact of network topology. This paper uses the transfer convenience index to characterize the transfer convenience and extracts the topological indicators, including the collinearity degree, from the URT networks of fifty global cities. Leveraging a back propagation neural network model integrated with SHAP, the study analyzes the transfer convenience and influencing factors of the URT network. Our findings reveal a threshold effect of the collinearity degree on transfer convenience. When the collinearity degree is disregarded, the relationship between the transfer convenience index and the number of transfer stations predominantly aligns with an exponential function model. When the transfer station number exceeds 15, the transfer convenience index reaches its maximum in a ring–radial morphology. The conclusion could help urban planners understand the changing rules of transfer convenience in the URT network, guiding strategic decisions on transfer station placement and network morphology selection.

Keywords: urban rail transit; network topology; transfer convenience; back propagation neural network; SHAP

check for updates

Academic Editors: Sara Moridpour and Zhenyu Mei

Received: 19 August 2025
Revised: 20 October 2025
Accepted: 3 November 2025
Published: 4 November 2025

Citation: Li, Q.; Zhu, Z.; Zhao, Y.; Zhang, X.; Hu, X.; Xiong, W. Research on the Impact of Urban Rail Transit Network Topology on Transfer Convenience: Evidence from 50 Cities Worldwide. *Sustainability* **2025**, *17*, 9821. https://doi.org/10.3390/su17219821

Copyright: © 2025 by the authors. Licensee MDPI, Basel, Switzerland. This article is an open access article distributed under the terms and conditions of the Creative Commons Attribution (CC BY) license (https://creativecommons.org/licenses/by/4.0/).

1. Introduction

Urban rail transit (URT) is an important mode of transport in modern metropolises, with advantages of safety, economy, environmental friendliness, and punctuality. As a crucial solution to escalating road congestion and environmental pollution, URT's role is becoming increasingly significant [1–3]. By the end of 2024, URT systems were operational in 562 cities in 79 countries around the world [4]. In China, for example, as of 31 December 2024, 290 URT lines have been operating in 58 cities in China, with a total operating mileage of 12,160 km, and the URT systems in cities such as Beijing, Shanghai, Guangzhou, and Shenzhen have entered into networked operation.

Transfer is prevalent during passengers' use of URT, and networked operations are often accompanied by an increase in the number of transfers and transfer flows [5–7]. For example, in the City of London rail network in the United Kingdom, about 44% of trips on weekdays have at least one transfer, of which 87% have one transfer and 12% have two transfers [8]. In the Beijing Metro network in China, more than 40 percent of passengers experience a transfer activity during their journey. Most transfers are quite complex due to the complexity of the infrastructure at the transfer stations and the large ridership. A survey

in Shanghai, China, showed that when passengers traveled in the metro system, about 50% of their travel time was usually taken up by the transfer process [9]. Therefore, inconvenient transfers in URT networks may affect their service levels and reduce passenger satisfaction, thus affecting the use of the URT by passengers in their choice of travel mode [10,11].

Due to the diversity of natural geological conditions, geographical patterns, land use planning, and passenger flow distribution, the forms of URT networks vary across cities. This variation results in differences in the layout of URT lines, stations, and transfer stations, as well as in the network's functions and operational efficiency. Based on theoretical frameworks for classifying urban rail transit network morphologies, scholars have identified up to 18 different structural types [12]. Research on network structures often employs graph-theoretic indicators to define three fundamental types: radial, grid, and ring–radial [13,14]. Complex network theory provides a quantitative basis for morphological classification from a topological perspective, validating the rationality of this structural categorization [15,16].

Through a geometric decomposition into radial, grid, and ring units [17], this study identifies four core network morphologies—radial, grid, ring–radial, and ring–grid, as illustrated in Figure 1. These four morphologies encompass the representative skeletal structures of mature global URT networks, ensuring comparability in transfer convenience [18,19].

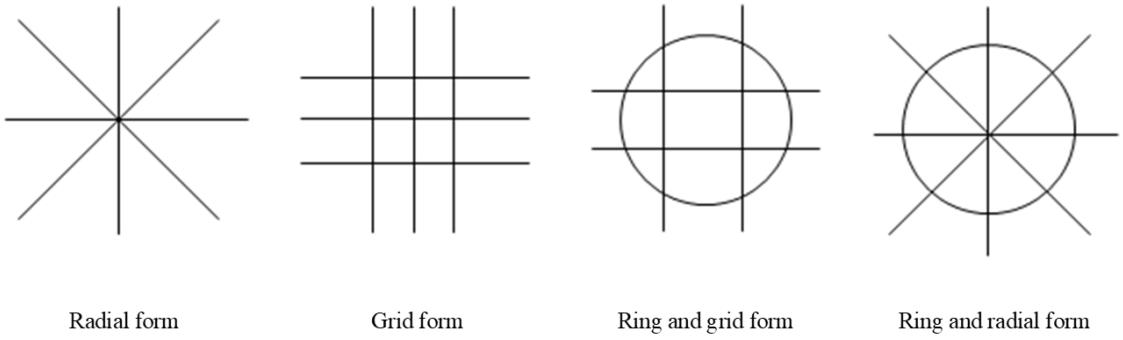


Figure 1. Four basic urban rail transit (URT) network morphologies.

In addition, the form of the line is also differentiated between intersecting form and colinear form [20,21], all of which will have an impact on the transfer convenience of the URT network. Studies have found that these two forms as distinct clusters with statistically significant differences, such as the ratio of transfer stations to lines [22]. The intersecting form is characterized by discrete transfer nodes, whereas the colinear form features continuous shared corridors, capturing fundamental differences in line operation and passenger transfer experience.

As shown in Figure 2, the basic feature of the intersecting form is that two rail lines are separated from each other at transfer stations. Two lines with a transfer relationship usually have one or more public transfer stations, which are often not continuous [23]. URT networks achieve relatively high network coverage with fewer lines, which facilitates rapid expansion of the network to cover major passenger corridors.

As shown in Figure 3, the basic characteristic of a colinear form is that two rail lines use parallel or shared tracks at transfer stations, where passengers transfer to the other line in the same or opposite direction at the same platform, and there are usually continuously available transfer stations along the line. Cities with this network form usually have a unique urban form and history. At the same time, not every line operates on a common line or common track [24]. During the construction and development of a colinear form network, a combination of colinear and intersection forms can be used to expand the network.

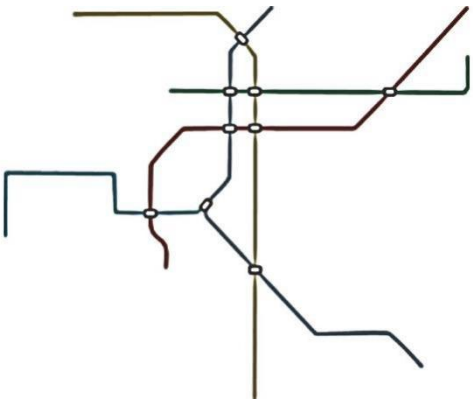


Figure 2. Intersection form of urban rail transit network.

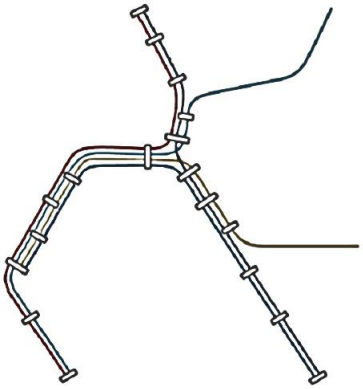


Figure 3. Colinear form of urban rail transit network.

Existing studies have demonstrated that collinearity in transit networks significantly affects transfer performance and system efficiency. Fan and Machemehl [25] showed that collinearity between routes influences passenger waiting behavior and transfer choices, thereby altering perceived accessibility. Derrible and Kennedy [26] found that excessive collinearity in global metro systems undermines network resilience and operational efficiency. Cats [27] analyzed the Stockholm metro, highlighting that collinear sections reshaped transfer opportunities and reduced system robustness. Jiang et al. [28] quantified navigation complexity in large-scale transit systems and revealed that higher collinearity increases passengers' cognitive burden, thus lowering transfer convenience.

Recent research has further emphasized route diversity and redundancy as critical dimensions of network performance. For example, Wang et al. [29] integrated route diversity and spare capacity to assess redundancy, while Li et al. [30] developed methods to evaluate route diversity by explicitly considering collinear segments of transit lines. Dixit [31] investigated the perception of collinearity in multimodal networks, showing that passengers often perceive highly collinear lines as functionally equivalent, which diminishes the effective benefits of multiple routes. In addition, resilience-oriented studies demonstrate that collinearity interacts with redundancy in shaping system continuity under disruptions [32].

Although scholars have conducted extensive research on transfers in URT, there is limited literature on the impact of URT network topology on transfer convenience. However, the URT network topology can determine the number of passenger transfers required during a journey, and frequent transfers can directly affect the traveling experience of passengers. In addition, URT systems are primarily located underground (i.e., part of an above-ground station) in the city. It is difficult to change the network structure after construction. Therefore, it is necessary to fully consider the difference in network

morphology in transfer capacity in the planning stage, and rationally select network morphology and operation mode to minimize the number of transfers and improve the transfer convenience.

In order to solve the above problems, this paper selects fifty URT networks in the world according to four network morphologies, extracts the transfer convenience indexes, and investigates the nonlinear effects of their influencing factors based on a back propagation neural network and SHapley Additive exPlanations algorithm. The main contributions of this paper are as follows:

(1) A transfer convenience index was used to characterize the transfer convenience in terms of the topology of the URT network.
(2) The relative importance and nonlinear effects of network topology parameters on the impact of transfer convenience are analyzed.
(3) Reveals the changing rules of transfer convenience under different network morphologies.

The remainder of the paper is organized as follows: Section 2 reviews previous studies on the subject. Section 3 describes the modeling methodology used, as well as the calculation of the collinearity degree and the transfer convenience index. In Section 4, we present and analyze the relationship between transfer convenience and network topology by investigating fifty URT systems around the world. Finally, Section 5 gives the main conclusions.

2. Literature Review

2.1. Research Related to Urban Rail Transit Network Topology

URT is a complex system, so it is possible to construct the URT network as a complex network. Graph theory and complex network theory have been gradually used in the study of topological features of URT networks. Several statistical studies have shown that the URT network has small-world network characteristics in general.

Based on graph theory, Gattuso et al. [33] investigated metro networks in 13 metropolitan areas through the use of geographical indicators. In contrast, Derrible et al. [34] investigated the relationship between patronage and network design (measured by three metrics, i.e., "coverage, accessibility, and connectivity") by using newer graph theoretic concepts, and concluded that the network topology plays a key role in attracting passengers to public transport. Latora and Marchiori [35] first introduced the complex network theory into metro research, and took the Boston metro network as an example, which proved that the metro network is a small-world network with scale-free characteristics. The results showed that the small-world effect in the space P model was more obvious than that in the space L model. As many transport systems are increasingly facing various service disruptions [36–38], scholars tend to construct topological indicators that can reflect the performance of traffic networks based on complex network theory [39–42].

Given that previous studies of transport network topology have focused on single-peak networks and that many cities have integrated public transport modes, Hong et al. [43] used a comprehensive public transport network in Seoul as an example, analyzed it using graph theory, and compared its characteristics with single-peak networks. The conclusions show that integration improves connectivity and spatial accessibility to inner-city suburbs. Shanmukhappa et al. [44] systematically summarized the latest developments in network theory for public transport network analysis using various network parameters for bus transport networks and metro transport networks in Hong Kong and London. The evaluated local and global characteristics provide a common platform to understand network characteristics in topological structures. Furthermore, recent research extended the analysis of network topology beyond single-mode URT systems to multi-layer regional railway networks (MRRNs) [45], highlighting the importance of network topology integration

not only at the urban scale for operational efficiency but also at the regional scale for socio-economic outcomes.

2.2. Research Related to the Urban Rail Transit Transfer Convenience

Based on the deepening knowledge of the rail network structure, many scholars have started to further study the transfer convenience of the URT network, which is a concern for passengers. Kim et al. [46] investigated the impact of the service level of transfer stations on people's travel choices based on the Rasch analysis, combined with the subjective perception of public transport users, and the results showed that services related to the transfer convenience, such as the walking facilities, the distance of walk, etc., are the key to encourage people to use URT. Wu et al. [47], in their study on the spatial environment of transfer stations, found that convenience and safety had a greater impact on the environmental suitability of the transfer space than utility, comfort, and aesthetics.

As a transfer station, transfer is its main function, so transfer efficiency is naturally its main evaluation factor [48–50]. Lee et al. [51] used data envelopment analysis (DEA) to estimate the transfer efficiency and performed a Tobit regression analysis to determine the factors affecting the transfer efficiency. The DEA model showed that the transfer efficiency score of a station is proportional to the number of transfers and the transfer rate. Some scholars have studied the transfer between rail stations and other modes of transportation [52–55], and the influence of train operation plan on transfer [56–59]. These studies tend to be conducted from the perspective of the station, and it is difficult to reflect the mechanism of the overall network structure on the transfer convenience.

Beyond the internal station design and operational factors, the broader multimodal transit-micromobility modes also shape transfer convenience [60,61]. Studies have shown that bike-sharing improves URT transfer convenience by solving the "last-mile" problem, with usage influenced by the spatial proximity to transit stops [62]. Moreover, it serves as a flexible feeder or alternative during disruptions, sustaining convenient transfer possibilities where URT service is limited or altered [63,64]. Other scholars have drawn attention to the equity concerns that may arise when improving network transfer convenience [65–67]. Kujala et al. [68] explored holistic accessibility analyses that integrate travel time, waiting time, and transfers. Furthermore, Zhu and Rui [69] examined the limitations of network expansion, finding that accessibility disparities may persist at finer spatial scales.

In summary, the literature review on the analysis of transfer convenience of URT networks in this paper shows that (1) most of the previous studies on the level of URT networks have focused on analyzing the network characteristics and evaluating the reliability of the rail transit networks, and the network parameters used have lacked the reflection of the transfer convenience of the URT networks. (2) Previous studies on transfer convenience mainly studied the evaluation and improvement of transfer efficiency of subway transfer stations from the perspectives of internal transfer facility design, train operation scheme, and transfer with other modes of transportation. However, few studies have focused on the relationship between the overall network topology of the URT and transfer. Nevertheless, from the perspective of affecting a passenger's one-time trip, the transfer convenience is not only determined by the transfer efficiency within the transfer station, but is also related to the network topology structure of the URT network.

While passenger-centric factors such as waiting time, walking distance, and comfort are crucial to the experience of transfer convenience, this study focuses on the underlying topological structure that enables or constrains such convenience. The network topology provides the foundational framework within which operational and behavioral factors operate. For this reason, this paper uses the transfer convenience index to study the transfer convenience of the URT network from the perspective of network topology.

3. Data and Methods

3.1. Data Collection and Processing

3.1.1. Data Sources

URT includes metro, light rail, monorail, tram, and other forms. Since transferring between different types of URT can be complex, and the metro system is the most widely used and constitutes the majority of URT, this paper focuses specifically on metro systems. The study examines the urban rail transit networks of 50 cities across 25 countries, including China and the United States. The selected cities all have networks with more than 100 stations or a total route length exceeding 100 km, ensuring a certain level of representativeness. The data were sourced from metro operation route maps provided by the official websites of local city metro companies as of April 2023.

3.1.2. Transfer Convenience Index

With the expansion of cities and the gradual networking of rail systems, it is difficult for passengers to complete a journey without transfer, and it is often necessary to transfer between lines [70,71]. Transfer refers to the act of passengers traveling between different lines and purchasing tickets again without leaving the paid area of the station [72]. In this study, a transfer station is defined as a node where passengers can switch between at least two different lines without exiting the fare-paid area, encompassing same-platform, cross-platform, and passageway-based transfers. A station is counted as a single transfer node irrespective of the number of lines converging at it. Firstly, setting up a certain number of convenient transfer stations increases the route choice of passengers, so that passengers can travel in a more flexible way. Secondly, transfer can balance the passenger flow and prevent the passenger load from being too high. In addition, transfer increases the flexibility and stability of network operation to a certain extent.

Transfer stations in URT networks increase the opportunities for line-to-line transfers and improve network accessibility [73]. In this paper, considering the transfer characteristics of URT networks, the transfer convenience index, K, is introduced as a new topological parameter to quantify the ease of transferring between different lines in an urban rail transit network from a structural perspective, and explore the difference in transfer convenience of URT networks with different network forms. A higher value of K indicates that passengers have more potential paths and greater flexibility when transferring between lines, which enhances the overall connectivity and convenience of the network. The number of transfer stations between any pair of distinct lines in the network is represented by a matrix of transfer opportunities as shown in Equation (1):

$$\begin{aligned} &D = (d_{ij})_{l\times l} \\ &d_{ij} = \begin{cases} \lambda_{ij} & i \neq j \\ 0 & i = j \end{cases}, \; i = 1,2,\cdots,l; j = 1,2,\cdots,l \end{aligned} \tag{1}$$

where λ_{ij} denotes the number of stations where direct transfer can be made between lines i and j, and l denotes the number of lines in the rail network.

The ratio of the sum of the elements in the matrix D to the number of lines in the network is defined as the transfer convenience index K, as shown in Equation (2):

$$K = (\sum_{i=1}^{l}\sum_{j=1}^{l} d_{ij})/l \tag{2}$$

The transfer convenience index, K, represents the average number of transfer connections per line in the network. Its unit is "number of transfer opportunities per line". A

higher K indicates that there are more available paths from one line to another and that the nearest transfer station can be selected. Thus, the higher the value of K for a network, the more convenient the transfer is at the network level.

As can be seen from Table 1, the K of each URT network has a large difference, fluctuating within the range of [2, 45.17], with the ratio of the highest to the lowest reaching 22. This wide range reflects the vast disparities in network connectivity and integration among the world's URT systems. There are some differences in K among different network morphologies. The average K of ring–radial is 14.07, which is higher than other network morphologies. There are also some differences in K of the same URT network morphology, among which, the ring–grid network has the smallest difference with a sample standard deviation of 2.44, and the K of radial and ring–radial networks have larger differences with a sample standard deviation of more than 10. The differences in transfer convenience values across different cities and network morphologies indicate the variations in the design and layout of urban rail transit systems across cities, which result in notable fluctuations in transfer convenience. In particular, the network topology plays a crucial role in influencing transfer convenience.

Table 1. Transfer convenience index under different network morphologies.

Network Morphology	Sample Size	Minimum	Maximum	Average	Standard Deviation
Radial	15	2	38	10.31	10.31
Grid	11	2	20.5	6.34	5.16
Ring–radial	13	3.33	45.17	14.07	10.86
Ring–grid	11	4.3	11.2	6.61	2.44

3.1.3. Network Topology Parameters

According to the different operation organization and transfer modes, the URT network is classified into intersection and colinear forms.

The URT network is considered to be colinear if there are two or more consecutive transfers in two or more lines in the network. The level of collinearity is referred to as the collinearity degree and denoted as r (expressed as a percentage in subsequent analyses for modeling consistency), as shown in Equation (3):

$$r = \sum_{L} \frac{1}{C_l^2} \cdot \frac{2m}{n_i + n_j}, r \in [0, 1) \tag{3}$$

where L denotes the number of groups of co-located rail lines, L = 1 if there are two co-located lines; l denotes the total number of URT lines; ${C_l}^2$ denotes the number of combinations of 2 elements taken out of l different elements; m denotes the number of consecutive transfer stations in two co-located lines; n_i denotes the number of stations on line i; n_j denotes the number of stations on line j.

The network topology parameters and descriptive statistics used in this study are shown in Table 2. The complete dataset of all 50 cities is provided in Table A1 of Appendix A. To isolate the effect of topology and enhance the comparability across the global sample, variables such as urban form, population density, and ridership patterns were not explicitly incorporated.

Table 2. Descriptive statistics of network topology parameters.

Variables	Meaning	Average	Standard Deviation
X_1	Number of lines	8.72	4.98
X_2	Number of stations	163.71	109.62
X_3	Number of transfer stations	26.66	19.65
X_4	Mileage (km)	240.81	200.09
X_5	Collinearity degree (%)	5.18	13.18

3.2. Methods

3.2.1. Back Propagation Neural Network

Back propagation neural network (BPNN) is a type of artificial intelligence technology inspired by the way neurons transmit stimuli and information to the brain. It offers advantages such as high accuracy of classification, strong parallel distributed processing capabilities, robust distributed storage and learning abilities, resilience to noisy inputs, fault tolerance, and the capacity to effectively approximate complex nonlinear relationships [74].

The BPNN consists of an input layer, a hidden layer, and an output layer, each of which has neurons connected using their weighting coefficients. The main operation process consists of two stages: forward propagation and transformation of the sample signal and backward feedback of the error, i.e., the input signal is normalized by the input layer and nonlinearly calculated by the hidden layer, and the corresponding output signal is generated by the output layer. The error is obtained by comparing with the actual output signal, and the weights and thresholds of the network are continuously adjusted by the backward propagation of the error, and the training of the network is finished when the obtained output results are within the predetermined error range, and the optimal weights of the input layer parameters are calculated by calling the weight matrix, as shown in Equations (4)–(6).

$$\begin{cases} r_{ij} = \sum_{k=1}^{p} w_{ki} \left(1 - e^{-x}\right) / \left(1 + e^{-x}\right) \\ x = w_{jk} \end{cases} \tag{4}$$

$$\begin{cases} R_{ij} = \left|\left(1 - e^{-y}\right) / \left(1 + e^{-y}\right)\right| \\ y = r_{ij} \end{cases} \tag{5}$$

$$S_{ij} = R_{ij} / \sum_{i=1}^{m} R_{ij} \tag{6}$$

where i is the neural network input unit, $i = 1, \ldots m$; j is the neural network output unit, $j = 1, \ldots, n$; k is the neural network implied unit, $k = 1, \ldots, p$; w_{ki} is the weight coefficient between the input layer neuron i and the implied layer neuron k; w_{jk} is the weight coefficient between the output layer neuron j and the implied layer neuron k; and S_{ij} is the weights of the parameters sought [75,76].

As the middle layer of the model structure, the hidden layer plays a crucial role in the model's operation. If the number of neurons in the hidden layer is too high, it can lead to overfitting; if it is too low, the model may be undertrained, which negatively impacts prediction performance. However, there is no ideal analytical formula for determining a reasonable number of nodes in the hidden layer, which is also a shortcoming of the BPNN in practical applications. In this paper, we first use the empirical Equation (7) to determine the approximate range of the number of neurons in the hidden layer and then carry out several trial calculations to determine the optimal number of neurons in the hidden layer.

$$N = \sqrt{m + n} + a \tag{7}$$

where N represents the number of neurons in the hidden layer, m represents the number of neurons in the input layer of the neural network, n represents the number of neurons in the output layer of the neural network, and a is a constant between 1 and 10.

3.2.2. Interpretation of the Model

Machine learning models can often achieve the required accuracy, but their application is often limited by the inability to rationally interpret the features of the model. Instead, SHapley Additive exPlanation (SHAP) is used to explain the output of the machine learning model. SHAP provides a method for estimating the contribution to each feature based on game theory and local interpretation [77]. The contribution of each feature to the model output is assigned based on its marginal contribution. The Shapley value is determined as follows:

$$\varphi_k = \sum_{z' \subseteq x'} \frac{|z'|!(M - |z'| - 1)!}{M!} \left[f_x(z') - f_x(z'/k) \right] \tag{8}$$

where φ_k is the contribution of feature k; M is the number of features; x denotes the data points; $|z'|$ is the number of non-zero entries in z', $z' \subseteq x$. f (x) is the output of the original model, which can be expressed as follows:

$$f(x) = g(x') = \varphi_0 + \sum_{k=1}^{K} \varphi_k x_k \tag{9}$$

where φ_0 is the base value that represents the output when all input parameters are missing, usually the mean of the target variable in all samples, and g (x') is the explanatory model.

3.2.3. Nonlinear Regression

In this paper, ExpDec and Poly2D were chosen to complement the nonlinear fitting. The expressions for both are shown in Equations (10) and (11), respectively.

$$Y = y_0 + a_1 e^{-X/a_2} + a_3 e^{-X/a_4} \tag{10}$$

$$Y = y_0 + a_1 X_1^2 + a_2 X_2^2 + a_3 X_1 + a_4 X_2 + a_5 X_1 X_2 \tag{11}$$

where Y is the dependent variable, X, X_1, X_2 are the independent variable, a_1, a_2, a_3, …, a_n are the regression coefficients, and y_0 is the regression constant. The coefficients a are also known as the partial regression coefficients or slope coefficients.

4. Results and Discussion

4.1. Modeling Adjustments

The layers of the neural network model are connected to each other through different types of excitation functions, where the input layer is connected to the hidden layer through a log-sigmoid function, the purelin function is selected between the hidden layer and the output layer, and the training function is selected as the trainlm function.

The BPNN model used in this study is a 3-layer structure, in which the input layer is 5 neuron nodes, representing X_1, X_2, X_3, X_4, X_5, respectively, and the output layer is 1 neuron node, which represents the transfer convenience index. Generally speaking, setting up more than one implicit layer will increase the algorithmic complexity, prolong the training time, and have little effect on improving the accuracy; therefore, the study used a single hidden layer. According to the empirical formula to determine the approximate range of the number of nodes in the implied layer [3,12], after many tests, as shown in Figure 4, the model achieved the lowest MSE (the mean square error) and a high R^2 value when the number of neurons in the implied layer was set to 9, indicating optimal predictive

accuracy without overfitting. Therefore, the number of neuron nodes was determined to be 9 in further analyses.

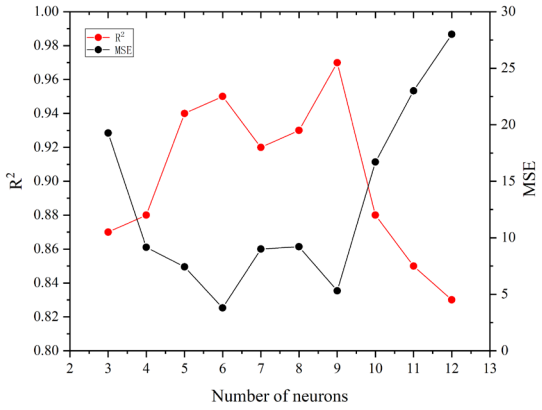


Figure 4. Determination of the number of neurons in BPNN.

4.2. Model Comparison

To test the robustness of the model, a comparative study was conducted between the operational results of BPNN and other machine learning methods, including Random Forest, Gradient Boosting, LightGBM, and a Graph Neural Network (GNN). Table 3 illustrates the outcomes. The BPNN model has lower RMSE and MAE values, and its R^2 value is also greater than the other models, indicating better fitting results, and supporting its suitability for capturing the complex nonlinear relationships in our topological dataset.

Table 3. Model comparison results.

	R^2	MAE	RMSE	CV R^2 Mean	CV R^2 Std
BPNN	0.6378	1.5440	2.2928	0.3891	0.2297
GNN	0.1258	3.0056	3.5621	−0.0060	0.2626
Random Forest	0.4235	2.1461	2.8927	0.4404	0.4700
Gradient Boosting	−0.7444	3.7463	5.0321	0.5314	0.3470
LightGBM	0.1368	3.3151	3.5396	−0.4547	0.9361

All analyses were conducted using Python 3.7 with key libraries including TensorFlow (for BPNN), scikit-learn (for comparative models), and PyTorch 1.13.1 (for GNN). A fixed random seed of 42 ensured reproducibility. The BPNN was trained for 100 epochs using the Adam optimizer (learning rate = 0.001). Comparative models were optimized via 5-fold cross-validation, and curve fitting utilized the Levenberg–Marquardt algorithm.

4.3. Relative Importance of Independent Variables

The results of the calculation of the importance of the independent variables to K are shown in Table 4. The ranking is based on the value of relative importance, with a sum of 100 percent. It can be seen that X_5 contributes the most to the prediction of the K, exceeding the sum of the other four variables at 51.94%, followed by X_3 (30.62%), which has a combined importance of more than 80%.

This paper further provides a more refined analysis of the possible influence mechanisms of the independent variables using the SHAP model, which generates a summary plot that ranks the independent variables according to their influence on K. In this plot, the x-axis represents the SHAP value (indicating the impact on the model output), and the color of the data points indicates the value of the independent variable—a redder value signifies that the actual value of the variable is larger within its respective range, such as mileage around 200 to over 800 km, number of transfer stations about 30 to 80, or degree of collinearity around 10% to 70%.

Table 4. Relative importance of independent variables.

Variable	Rank	Relative Importance (%)
X_1	4	5.21
X_2	5	4.79
X_3	2	30.62
X_4	3	7.44
X_5	1	51.94

As shown in Figure 5, the reddest points, which correspond to networks with exceptionally high collinearity, are clustered exclusively in the region of high positive SHAP values. When X_5 is higher, the SHAP value is higher, and there is a strong positive correlation with the K, and as X_5 decreases, the SHAP value gradually decreases, and there is even a negative correlation with the K, which shows that there is a threshold effect of X_5 on the K. This suggests that a collinearity degree exceeding a certain level is a key differentiator for high transfer convenience.

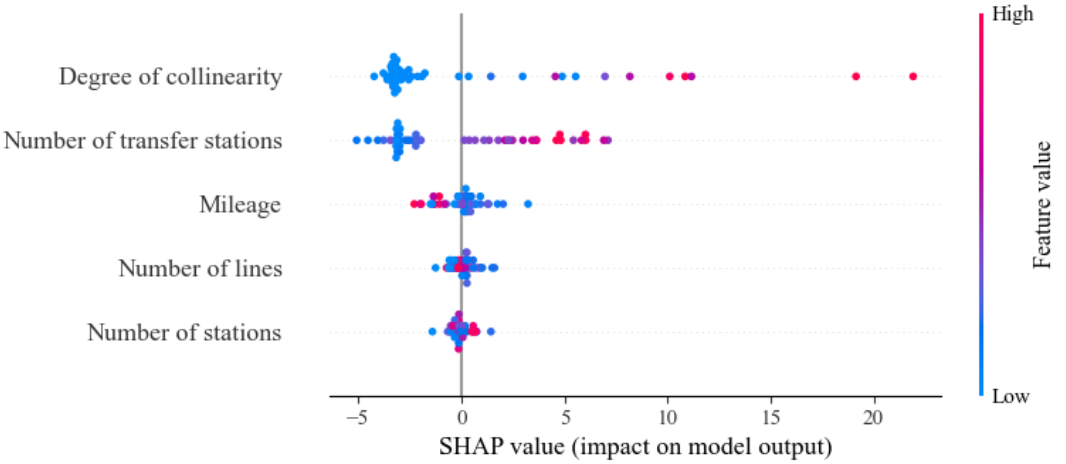


Figure 5. SHAP values of the independent variables for the transfer convenience index (K).

In contrast, the influence of X_3 on K is more complicated, and it can be seen that the SHAP value of the number of transfer stations increases and then decreases as the color becomes red. This pattern indicates that beyond a certain scale, merely increasing the number of transfer stations does not uniformly yield higher convenience. Therefore, the X_3, X_5, and K do not have a simple linear relationship, and more in-depth research is needed. The influence of other factors, such as the mileage and the number of lines, is comparatively lower, as their SHAP values are clustered closer to zero.

To further elucidate the nonlinear influence of the collinearity degree (X_5) identified by the SHAP analysis, a partial dependence plot (PDP) was employed. As can be seen from Figure 6, the PDP reveals a clear stepwise pattern: K increases steeply at collinearity thresholds of approximately 2%, 11%, and 18%, with stable plateaus observed between these points. Additionally, the grey bars delineates the density distribution of collinearity degree, with peaks around 0 and 17.5 highlighting the most prevalent levels. This demonstrates the discontinuous nonlinear impact of collinearity on transfer convenience and provides critical insights for staged network design.

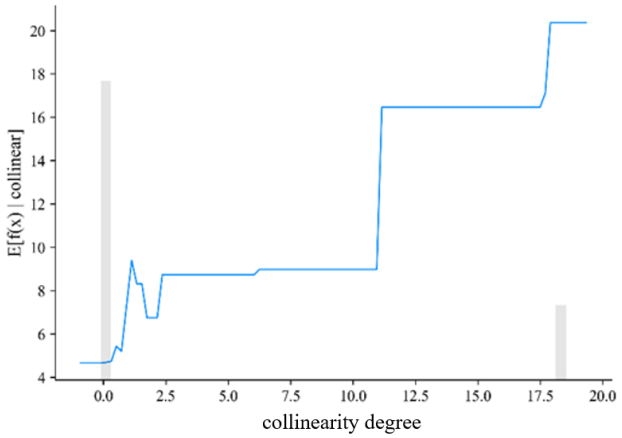
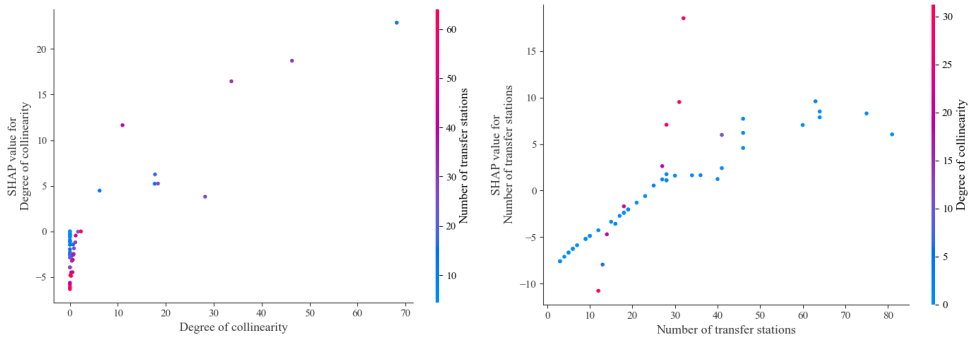


Figure 6. Partial dependence plot for the collinearity degree.

4.4. Interaction Between Collinearity Degree and the Number of Transfer Stations

In order to further reveal the mechanism of the influence of the X_3 and X_5 on the K, we used BPNN and SHAP to obtain the influence of the interaction between the X_3 and X_5 on the K, as shown in Figure 7. This interaction is further visualized in the updated Figure 8 via a heatmap and a 3D surface plot. X_3 and X_5 as the independent variables and K as the dependent variable were fitted using Poly2D, and the fitting results are shown in Equation (12).



(**a**) (**b**)

Figure 7. SHAP values of collinearity degree (X_5) and number of transfer stations (X_3): (**a**) SHAP values of collinearity degree (X_5). (**b**) SHAP Value of number of transfer stations (X_3).

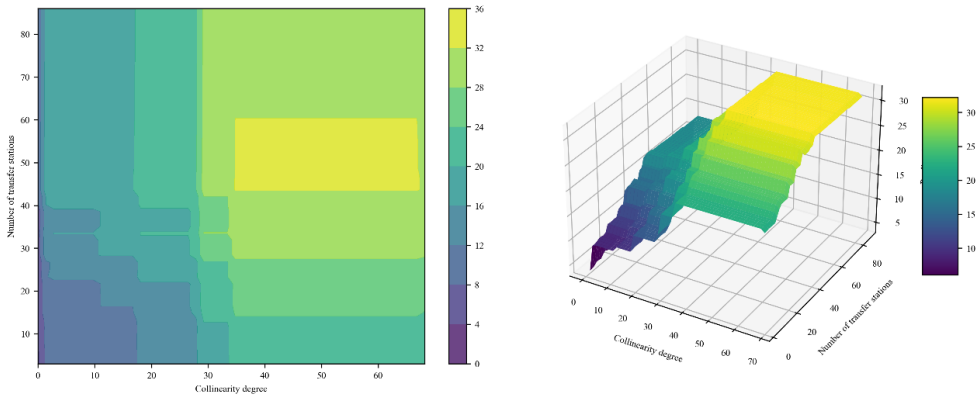


Figure 8. Interactions of collinearity degree (X_5) and number of transfer stations (X_3).

As shown in Figure 7a, the larger the collinearity degree, the larger the SHAP value, and when X_5 exceeds 10%, the SHAP value is generally greater than 0. Meanwhile, Figure 7b shows that X_5 can significantly change the influence of X_3 on K, and the higher the X_5, the higher the SHAP value of X_3. Combined with Equation (13), it can be obtained

that for every 1% increase in X_5, the increase in X_3 for K increases by 0.03 for every increase in X_3. Therefore, in the planning of the line network, especially when the URT network reaches a certain scale and the increase in the number of transfer stations for the increase in K is already very weak, it can be further improved by adopting the colinear form to improve K of the URT network. The transfer convenience of the URT network can be further improved by adopting the colinear form.

$$T = 1.35 - 0.002X_3^2 - 0.003X_5^2 + 0.278X_3 - 0.07X_5 + 0.03X_3X_5 \quad (12)$$

$$\begin{cases} T'_{X_3} = 0.278 - 0.004X_3 + 0.03X_5 \\ T'_{X_5} = -0.07 - 0.006X_5 + 0.03X_3 \end{cases} \quad (13)$$

These interaction patterns are further visualized in Figure 8. As shown in the heatmap, the influence of the number of transfer stations (X_3) on K intensifies markedly as X_5 increases. Complementarily, the 3D surface plot directly illustrates how the effect of X_3 is modulated by X_5, showing that the marginal contribution of transfer stations to convenience is elevated within a high-collinearity context.

4.5. Impact of the Number of Transfer Stations on Transfer Convenience

The number of transfer stations is an important factor affecting K. The more transfer stations there are, the more transfer nodes connecting different lines, the more traveling paths passengers can choose, and the better the transfer convenience. The SHAP analysis revealed that the collinearity degree (X_5) is the most dominant factor influencing K and exhibits a complex interaction with X_3. To minimize this confounding effect and to better isolate and capture the underlying relationship between X_3 and K that is not driven by extreme collinearity, 12 cities with large X_5 were excluded from this specific analysis. We used BPNN and an exponential function to fit the functional relationship between the two; the trend is shown in Figure 7, and the values of the fitted parameters, including the goodness-of-fit measures R^2, Adjusted R^2, MAE, and RMSE, are summarized in Table 5. These metrics consistently confirm the superior performance of the BPNN model.

Table 5. Fitting results of different functions.

Model	Fit the Results				Parameter Estimates				
	R^2	Adjusted R^2	MAE	RMSE	Constant	a_1	a_2	a_3	a_4
BPNN	0.86	0.85	1.26	1.66					
ExpDec	0.81	0.78	2.24	2.89	13.38	−4.41	2.41	−10.58	60.99

The parameter constant (denoted as y_0) represents the asymptotic maximum value of K when X_3 is very large. The coefficients a_1 and a_3 indicate the initial deviations from this maximum, while a_2 and a_4 are decay constants that determine how rapidly K approaches y_0 as X_3 increases.

As can be seen from Figure 9, with the increase in X_3, the overall trend of K is increasing. The R^2 value of the fitting using BPNN is 0.86, which is significantly better than the fitting effect of the exponential function. As shown in Figure 9a, when X_3 is in the ranges of 0–15, 21–30, 65–75, K has a significant increase, and there is a long period of stabilization when it is between 30 and 65. As shown in Figure 9b, with the increase in X_3, the increase in K slows down, and when X_3 reaches 35 or more, each additional transfer station can only improve K by 0.1. Therefore, when planning the line network, it is necessary to set up a reasonable number of transfer stations. When the number of transfer stations is less than 30, it is necessary to increase the number of transfer stations to improve the convenience of the URT network. When the number of transfer stations reaches more than 35, it is unwise to

blindly increase the number of transfer stations, because this strategy does not sufficiently help to improve the convenience of the URT network. At the same time, we can see that with the increase in X_3, the degree of discrete points gradually increases.

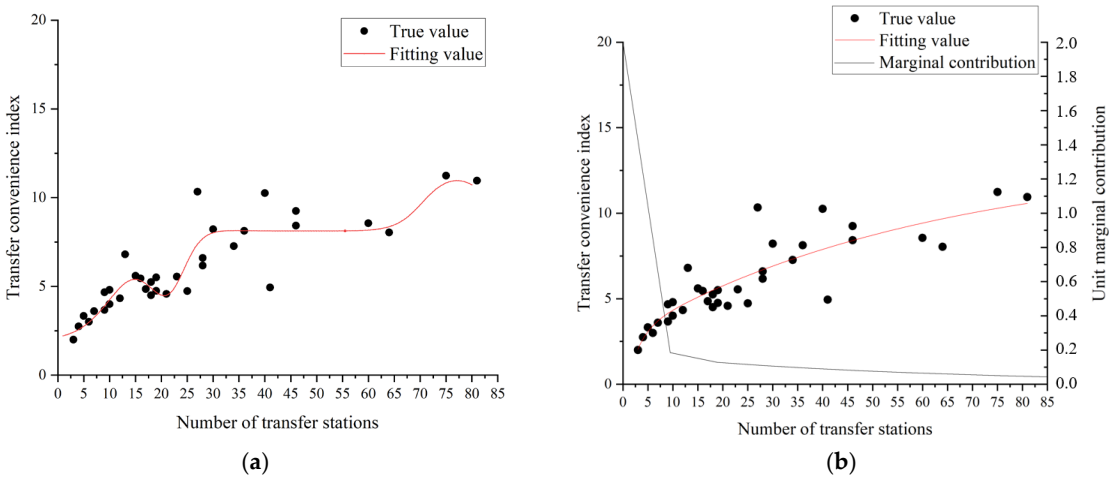


Figure 9. Relationship between transfer convenience index (K) and the number of transfer stations (X_3): (**a**) BPNN; (**b**) ExpDec.

Therefore, to quantitatively investigate this changing relationship, we calculated the Pearson correlation coefficient between X_3 and K as X_3 increased, along with its 95% confidence bands. As shown in Figure 10, when X_3 is lower than 15, K shows a significant correlation with X_3, while the correlation weakens with the increase in X_3. The possible reason for this is that when X_3 is small, the relationship between K and X_3 is similar under different network morphologies, but with the increase in line density, the network morphologies are basically fixed, which makes the relationship between K and X_3 more complicated.

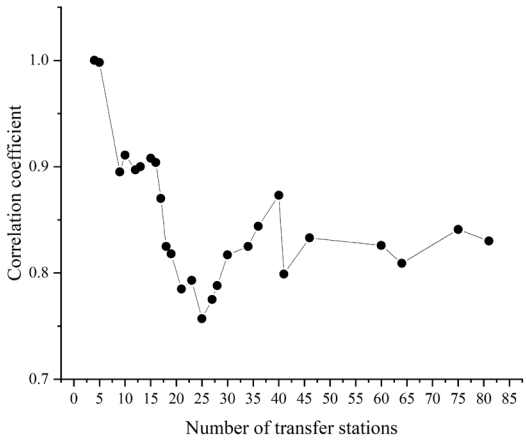


Figure 10. The Pearson correlation coefficient vs. the number of transfer stations.

It is important to note that the exponential relationship identified between X_3 and K is derived from networks with low to moderate collinearity. Consequently, the findings and planning implications may not be directly generalizable to systems with high degrees of collinearity. In such networks, the presence of shared corridors fundamentally alters the transfer dynamics, and the convenience is more significantly enhanced by the collinearity degree itself.

4.6. Impact of Network Morphology on Transfer Convenience

This paper investigates changes in transfer convenience after removing different proportions of the number of nodes from URT networks with different morphologies. To explore general patterns, cities with extensive co-locations were not considered. The nodes with the largest degree play an important role in the network, making the network vulnerable to attacks targeting these nodes with the largest degree. Therefore, in this paper, after removing one node with the largest degree in the network, we calculated the K of the remaining network once until the K of the network was 0 and obtained the relationship between the K and the proportion of removed points under different network morphologies, as shown in Figure 11.

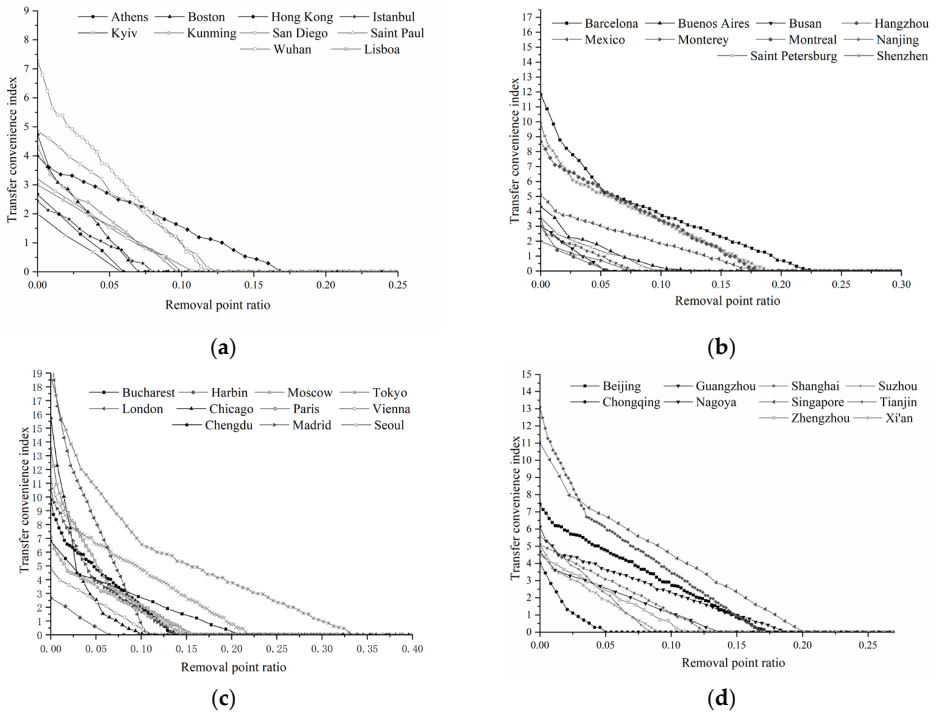


Figure 11. The relationship between the transfer convenience index (K) and the removal point ratio for 4 URT morphologies: (**a**) radial; (**b**) grid; (**c**) ring–radial; (**d**) ring–grid.

Figure 11a shows the variation in K of the radial network, and it can be seen that K basically shows a linear decrease with the increase in the proportion of removed points. When the proportion of removed points reaches 10%, the K basically decreases to zero. Figure 11b shows the change in K of the grid network. Compared with the radial network, the decreasing trend of K is slowed down, and the robustness of the network is relatively enhanced. When the proportion of removed points is around 10% versus 18%, the K basically drops to zero. Figure 11c shows the variation in K of the ring–radial network, and the K is significantly improved compared to the radial network. With the increase in the proportion of removed points, the decrease in K gradually decreases, and at the same time, the higher the K, the smaller its decrease, i.e., the more robust the network is. As shown in Figure 11d, the overall K of the ring–grid network is higher than that of the grid network, and its variation is similar to that of the grid network.

Through previous exploration, we have found that the exponential function better describes the relationship between the two variables. To further investigate the impact of network morphology on transfer convenience, we used the exponential function to fit the relationship between K and X_3 in the URT network across different network morphologies. The fitting results are shown in Figure 10 and Table 6.

Table 6. Fitting results under different network morphologies.

Network Morphology	Fit the Results				Parameter Estimates				
	R^2	Adjusted R^2	MAE	RMSE	Constant	a_1	a_2	a_3	a_4
Radial	0.91	0.83	2.34	3.26	46.35	−22.04	446.07	−21.82	235.81
Grid	0.96	0.84	1.16	1.53	15.69	−5.27	2.21	−12.72	96.47
Ring–radial	0.95	0.84	2.07	2.39	44.46	−7.94	9.35	−36.79	865.37
Ring–grid	0.95	0.81	0.68	0.65	58.48	−26.94	573.18	−28.28	550.69

When the relationship between X_3 and K is fitted after classifying different network morphologies, the R^2 value reaches more than 0.9, which indicates that the network morphology also affects the transfer convenience, and there are different morphologies between X_3 and K under different network morphologies. The low MAE and RMSE values further confirm the robustness of these fits. Among them, the R^2 of the grid network reaches 0.96, but also low errors, which indicates that the change of the K is the most stable under the grid network morphology. Notably, the ring–grid morphology exhibits the smallest prediction errors, underscoring its structure and the highly predictable relationship between transfer stations and convenience.

Meanwhile, Figure 12 shows that under the same condition of X_3, the ring–radial network has the largest K. When X_3 is more than 10, the radial network can significantly improve K by adding loop lines, while the grid network will only produce certain benefits for the K when X_3 reaches more than 20. Therefore, in the long-term planning of the URT network, the choice of a ring–radial network can better improve the transfer convenience of the URT network.

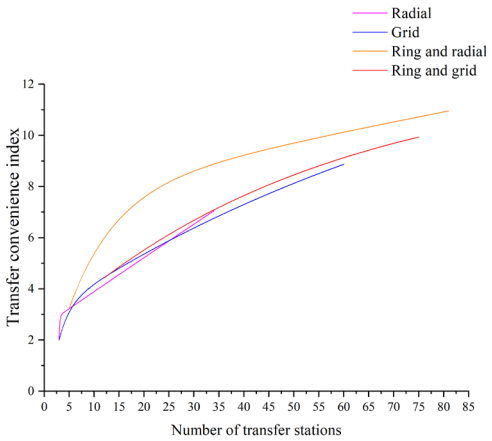


Figure 12. Exponential function fitting of K vs. X_3 with different network morphologies.

5. Conclusions

5.1. Summary and Major Findings

This research delves into the impact of network topology and morphology on transfer convenience in URT systems, shifting the analysis of transfer convenience impacts from the station level to the network level. Through an analysis of 50 global URT networks, our study confirms the hypothesis that network topology and collinearity significantly influence transfer convenience for URT passengers. The study employs regression analysis to elucidate the relationship between the transfer convenience index and network topology. Key conclusions are as follows:

Collinearity degree and the number of transfer stations emerge as pivotal factors influencing URT transfer convenience. The collinearity degree can significantly affect the relationship between the number of transfer stations and the convenience index. There-

fore, we suggest that the design of common lines should be reasonably adopted in the construction of URT to improve the transfer convenience of the network.

Excluding collinearity considerations, a nearly exponential relationship is discernible between the transfer convenience index and the number of transfer stations. However, the marginal benefit of adding transfer stations diminishes beyond a certain point, particularly when the number exceeds 35. This finding underscores the need for strategic planning in URT expansion, avoiding indiscriminate increases in transfer stations.

Network morphology also plays a vital role in shaping transfer convenience. When the number of transfer stations is more than 15, the change of transfer convenience in different network morphologies starts to diverge, with the ring–radial configuration demonstrating superior convenience. These findings have a certain significance, and decision-makers should pay more attention to the network morphology when planning and designing the URT network.

5.2. Policy Implications

Beyond the theoretical and empirical findings, this study provides several policy-oriented insights for the planning and management of urban rail transit (URT) systems. These implications are intended to guide decision-making in both established and rapidly developing cities, ensuring that infrastructure investments are not only technically sound but also socially and economically sustainable.

Firstly, for cities with predominantly radial networks, the collinearity degree and the number of transfer stations should guide long-term development strategies. When transfer stations exceed 10, planners should begin preparing for circumferential connections. Policy measures may include reserving land corridors for future ring lines, incorporating ring components in master plans, and prioritizing ring–radial expansion in medium- and long-term investment programs. Institutional coordination between municipal and regional planning agencies is essential to ensure that ring line projects align with population growth and demand forecasts.

Moreover, the diminishing marginal returns of transfer stations beyond 35 highlight the need for investment rationalization. Our analysis shows that while adding transfer stations initially expands passenger route options and significantly improves transfer convenience, the incremental benefit declines once a certain density is reached. Beyond this threshold, additional hubs tend to duplicate existing connections, concentrate flows, and increase operational complexity without yielding proportional gains in accessibility. This implies that investments should not simply target the number of transfer nodes, but rather focus on improving their quality and efficiency. Policymakers are therefore encouraged to apply cost–benefit evaluation frameworks when considering new transfer stations, taking into account projected demand, construction costs, and system-wide effects. Complementary measures—such as expanding the capacity of existing hubs, enhancing wayfinding and guidance systems, or deploying digital solutions like integrated ticketing and smart subsidies—can often deliver greater improvements to passenger experience than building additional stations.

In addition, collinearity should be explicitly considered in network design standards. Moderate collinearity can improve connectivity, but excessive overlap must be avoided. Policy actions can include setting upper thresholds for permissible line overlap during feasibility studies, requiring that environmental and social impact assessments address redundancy risks, and establishing design guidelines that encourage diversification of alignments in new lines. In addition, transport authorities can introduce evaluation tools that quantify passenger cognitive burden and operational vulnerability, ensuring that system efficiency is not undermined by redundant infrastructure.

Finally, the mechanisms identified in this study extend to multimodal systems, which require integrated governance. Policies should encourage coordinated planning between metro, light rail, tram, and bus systems to minimize transfer penalties. Recommended measures include the development of multimodal hubs that physically collocate different modes, synchronized scheduling across operators, unified ticketing and fare capping policies, and real-time multimodal information platforms. Moreover, when planning expansions, scenario-based planning tools should be employed: for example, prioritizing new transfer nodes when station density is low, and restructuring morphology toward ring–radial configurations when density is high. These measures will allow decision-makers to embed resilience and efficiency into multimodal networks.

5.3. Limitations and Future Research

Despite these findings, the study acknowledges its limitations. Firstly, urban rail network morphology is complex due to factors including urban form and land use, and therefore, the four classifications of URT networks used in the study may not describe all network morphology. Employing data-driven methods would enable more nuanced classifications that capture hybrid and evolving network characteristics. Secondly, while the research focused on global network topological parameters, the impact of local network characteristics remains an area for future exploration to aid in more nuanced urban rail network planning and design. Thirdly, the exclusion of high-collinearity networks in the exponential model analysis may affect its generalizability. Additionally, the study's scope is confined to metro systems and relies on static network maps, which do not capture dynamic operational elements like peak-hour demand or service disruptions. Future research could incorporate more sophisticated modeling techniques and extend the analysis to multimodal systems and dynamic data sources, providing a more unified understanding of these interconnected factors.

Furthermore, the transfer convenience index (K) is based solely on topological features and does not incorporate behavioral or operational factors. Future studies should build upon this topological foundation by integrating multi-dimensional passenger data to develop a more holistic understanding. Specifically, research could focus on (1) correlating topological indices with revealed passenger preferences from smart card data and stated preferences from passenger surveys; (2) investigating how operational factors like waiting time and crowding moderate the relationship between topology and perceived convenience; and (3) exploring how urban morphology interacts with network structure in shaping transfer efficiency. Integrating equity and accessibility perspectives remains a vital dimension for comprehensively evaluating network improvements. Such integrated approaches would bridge the gap between network structure and passenger experience, enabling more comprehensive planning frameworks for urban rail transit systems.

Author Contributions: Data curation, Q.L. and Z.Z.; Formal analysis, Q.L. and Z.Z.; Methodology, Q.L. and Y.Z.; Validation, W.X. and X.H.; Visualization, Q.L. and X.Z.; Writing—original draft, Q.L. and Y.Z.; Writing—review and editing, Z.Z. and W.X. All authors have read and agreed to the published version of the manuscript.

Funding: This work was supported by the Young Scientists Fund of the National Natural Science Foundation of China [grant numbers No. 52402385]; the Scientific Research Foundation for Advanced Talents of Nanjing Forestry University [grant numbers 163106041]; Postgraduate Research & Practice Innovation Program of Jiangsu Province [grant numbers SJCX24_0405]; and Postgraduate Research & Practice Innovation Program of Jiangsu Province [grant numbers KYCX23_1155].

Institutional Review Board Statement: Not applicable.

Informed Consent Statement: Not applicable.

Data Availability Statement: Some or all data, models, or codes that support the findings of this study are available from the corresponding author upon reasonable request.

Conflicts of Interest: Author Yunpeng Zhao was employed by the Qingdao Train Depot of China Railway Jinan Bureau Group Co., Ltd. Author Xuhui Zhang was employed by the Nanjing Metro Group Co., Ltd. The remaining authors declare that the research was conducted in the absence of any commercial or financial relationships that could be construed as a potential conflict of interest.

Appendix A

Table A1. Network topology parameters and transfer convenience index of URT networks across 50 cities.

Network Morphology	City	Number of Lines	Number of Stations	Number of Transfer Stations	Mileage (km)	Degree of Collinearity (%)	Transfer Convenience Index
Radial form	Amsterdam	5	39	18	42.7	17.75	15.2
	Athens	3	67	5	86.6	0	3.33
	Boston	5	143	10	117.7	0	4
	Brasilia	2	24	12	41	68.18	12
	Hong Kong	11	125	25	228	1.69	4.73
	Istanbul	10	141	28	208.2	0	6.6
	Kyiv	3	52	3	67.6	0	2
	Kunming	6	114	9	184.1	0	3.67
	Lisboa	4	56	6	44.5	0	3
	Munich	8	100	41	103	10.97	27
	Saint Paul	11	151	16	326.7	0.64	5.45
	San Diego	7	136	17	139.7	0	4.85
	San Francisco	5	46	31	167	46.33	38
	Washington	6	91	27	171	18.37	17.6
	Wuhan	11	291	34	460	0.71	7.27
Grid form	Barcelona	12	206	19	166	0	5.5
	Brussels	4	59	28	49.9	28.2	20.5
	Buenos Aires	6	86	9	54	0	4.67
	Busan	4	114	6	116.5	0	3
	Hangzhou	12	254	46	610.52	0.59	8.42
	Mexico	12	162	28	226.5	0	6.17
	Monterey	3	40	3	32	0	2
	Montreal	4	73	4	69.2	0	2.75
	Nanjing	12	208	21	449	0	4
	Saint Petersburg	5	72	7	124.8	0	3.6
	Shenzhen	11	283	60	529	0	8.56
Ring and grid form	Bucharest	5	62	13	78.5	6.18	6.8
	Chengdu	12	333	46	518.5	0	9.25
	Chicago	8	139	28	170.6	1.12	18.25
	Copenhagen	4	39	14	38.2	17.68	10
	Harbin	3	62	5	78	0	3.33
	London	12	275	46	408	1.2	21.22
	Madrid	12	301	40	294.8	0	10.25
	Moscow	15	270	36	420	0.76	8.13
	Oslo	6	105	32	84.2	33.68	45.17
	Paris	16	308	64	226.9	0.54	16.21
	Seoul	19	376	81	314	0.09	10.95
	Tokyo	15	285	63	304.1	2.3	18.57
	Vienna	5	98	10	83.3	0	4.8
Ring and radial form	Beijing	24	428	64	727	0	8.04
	Chongqing	9	208	30	387.7	0.39	8.22
	Guangzhou	18	213	41	783.1	0.27	4.94
	Nagoya	6	87	12	93.3	0	4.33
	Shanghai	20	508	75	831	0.23	11.24
	Singapore	6	134	27	230.6	0.85	10.33
	Suzhou	5	169	15	210	0	5.6
	Taipei	8	131	19	146.2	0	4.75
	Tianjin	9	181	23	286	0.25	5.55
	Xi'an	8	176	18	279	0	5.25
	Zhengzhou	8	164	18	232.5	0	4.5

References

1. Fara, A.A.; Graham, J.G.D.; Laila, A.; Ramandeep, S. Performance of urban rail transit: A review of measures and interdependencies. *Transp. Rev.* **2023**, *43*, 698–725. [CrossRef]
2. Deng, K.; Li, L. Rail transit and the growth of consumer amenities: Evidence from Chinese cities. *Transportation* **2023**, *51*, 1611–1634. [CrossRef]
3. Jiao, L.D.; Luo, F.L.; Wu, F.Y.; Zhang, Y.; Huo, X.S.; Wu, Y. Can the opening of urban rail transit improve urban air quality? Evidence from 94 lines in China. *Environ. Impact Assess. Rev.* **2022**, *97*, 106857. [CrossRef]
4. Han, B.; Li, Z.; Jin, Y.; Lu, F.; Hu, J.; Huang, S.; Wang, D.; Zhang, Z.; Gao, J.; Feng, F.; et al. A review of the 2024 global urban rail transit operation statistics and analysis. *Urban Rapid Transit.* **2025**, *38*, 1–12. (In Chinese) [CrossRef]
5. Chen, Y.; Mao, B.H.; Bai, Y.; Li, Z.J. Timetable synchronization of last trains for urban rail networks with maximum accessibility. *Transp. Res. Part C Emerg. Technol.* **2019**, *99*, 110–129. [CrossRef]
6. Wang, Y.; Qin, Y.; Guo, J.Y.; Jia, L.M.; Wei, Y.; Pi, Y.N. Multiposition Joint Control in Transfer Station Considering the Nonlinear Characteristics of Passenger Flow. *J. Transp. Eng. Part A Syst.* **2021**, *10*, 04021068. [CrossRef]
7. Hu, Y.T.; Li, S.K.; Dessouky, M.M.; Yang, L.X.; Gao, Z.Y. Computationally efficient train timetable generation of metro networks with uncertain transfer walking time to reduce passenger waiting time: A generalized benders decomposition-based method. *Transp. Res. Part B Methodol.* **2022**, *163*, 210–231. [CrossRef]
8. Guo, Z.; Wilson, N.H.M. Assessing the cost of transfer inconvenience in public transport systems: A case study of the London Underground. *Transp. Res. Part A Policy Pract.* **2010**, *45*, 91–104. [CrossRef]
9. Yang, L.X.; Zhang, Y.; Li, S.K.; Gao, Y. A two-stage stochastic optimization model for the transfer activity choice in metro networks. *Transp. Res. Part B Methodol.* **2016**, *83*, 271–297. [CrossRef]
10. Li, J.M.; Xu, X.Y.; Yao, Z.X.; Lu, Y. Improving service quality with the fuzzy TOPSIS method: A case study of the Beijing rail transit system. *IEEE Access* **2019**, *7*, 114271–114284. [CrossRef]
11. Wandelt, S.; Sun, X. Lufthansa Express Rail in Germany: A critical evaluation of benefits and limitations of the intermodal network based on journey time and fares. *Multimodal Transp.* **2022**, *4*, 100048. [CrossRef]
12. Gu, B.N.; Cao, Z.M. Study on the Network Structure of Urban Rail Transit. *J. China Railw. Soc.* **2000**, 25–29. (In Chinese) [CrossRef]
13. Derrible, S.; Kennedy, C. Characterizing metro networks: State, form, and structure. *Transportation* **2010**, *37*, 275–297. [CrossRef]
14. Yu, X.Y.; Chen, Z.; Liu, F.; Zhu, H.H. How urban metro networks grow: From a complex network perspective. *Tunn. Undergr. Space Technol.* **2023**, *131*, 104841. [CrossRef]
15. Owais, M.; Ahmed, A.S.; Moussa, G.S.; Khalil, A.A. An Optimal Metro Design for Transit Networks in Existing Square Cities Based on Non-Demand Criterion. *Sustainability* **2020**, *12*, 9623. [CrossRef]
16. Li, Z.M. A classification method of development stages in urban rail transit network. In Proceedings of the Second International Conference on Electronic Information Engineering, Big Data, and Computer Tech-nology (EIBDCT 2023), Xishuangbanna, China, 6–8 January 2023. [CrossRef]
17. Zhang, J.; Zhao, M.W.; Liu, H.; Xu, X.W. Networked characteristics of the urban rail transit networks. *Phys. A Stat. Mech. Its Appl.* **2013**, *392*, 1538–1546. [CrossRef]
18. Saidi, S.; Wirasinghe, S.C.; Kattan, L. Long-term planning for ring-radial urban rail transit networks. *Transp. Res. Part B Methodol.* **2016**, *86*, 128–146. [CrossRef]
19. Chen, P.W. Research on the Scheme Comparison of Xuzhou Urban Rail Transit Network Based on Network Form. *J. Phys. Conf. Ser.* **2023**, *2491*, 012010. [CrossRef]
20. Derrible, S.; Kennedy, C. The complexity and robustness of metro networks. *Phys. A Stat. Mech. Its Appl.* **2010**, *389*, 3678–3691. [CrossRef]
21. Massobrio, R.; Cats, O. Topological assessment of recoverability in public transport networks. *Commun. Phys.* **2024**, *7*, 108. [CrossRef]
22. Ma, Y.F.; Sallan, J.M.; Lordan, O. Rail Transit Networks and Network Motifs: A Review and Research Agenda. *Sustainability* **2024**, *16*, 3641. [CrossRef]
23. Kim, M.E.; Kim, E. Simulation-Based Multistage Optimization Model for Railroad Alignment Design and Operations. *J. Transp. Eng. Part A Syst.* **2020**, *146*, 04020057. [CrossRef]
24. Xu, S.T.; Gao, T.C.; Yang, D.Y.; Feng, X.Y.; Schonfeld, P.; Li, H.L.; Zhu, Y.; Wang, P.; He, Q. Energy-saving design of underground metro vertical alignment with deep reinforcement learning. *Tunn. Undergr. Space Technol.* **2024**, *149*, 105803. [CrossRef]
25. Fan, W.; Machemehl, R.B. Do transit users just wait for buses or wait with strategies? Some numerical results that transit planners should see. *Transp. Res. Rec.* **2009**, *2111*, 169–176. [CrossRef]
26. Derrible, S.; Kennedy, C. Applications of Graph Theory and Network Science to Transit Network Design. *Transp. Res. Rec.* **2011**, *31*, 495–519. [CrossRef]
27. Cats, O. Topological evolution of a metropolitan rail transport network: The case of Stockholm. *J. Transp. Geogr.* **2017**, *62*, 172–183. [CrossRef]

28. Jiang, Z.; Yang, J.; Luo, Y.; Zheng, S.; Hu, S. Quantifying navigation complexity in transportation networks. *PNAS Nexus* **2022**, *1*, pgac126. [CrossRef]
29. Wang, X.; Wang, L.; Zhou, X. Assessing transportation network redundancy by integrating route diversity and spare capacity. *Transp. A Transp. Sci.* **2023**, *19*, 1031–1053. [CrossRef]
30. Li, Y.; Zhou, J.; Chen, F. Measuring route diversity in spatial and spatio-temporal public transport networks. *Transp. Policy* **2024**, *146*, 42–58. [CrossRef]
31. Dixit, M. Perception of overlap in multimodal urban transit route choice. *Transp. A Transp. Sci.* **2023**, *19*, 239–260. [CrossRef]
32. Zhang, H.; Liu, Y.; Zhao, X. Improving transit network resilience against disruptions through path redundancy. *Socio-Econ. Plan. Sci.* **2025**, *93*, 101783. [CrossRef]
33. Gattuso, D.; Miriello, E. Compared analysis of metro networks supported by graph theory. *Netw. Spat. Econ.* **2005**, *5*, 395–414. [CrossRef]
34. Derrible, S.; Kennedy, C. Network analysis of world subway systems using updated graph theory. *Transp. Res. Rec.* **2009**, *2112*, 17–25. [CrossRef]
35. Latora, V.; Marchiori, M. Is the Boston Subway a small-world network? *Phys. A Stat. Mech. Its Appl.* **2002**, *314*, 109–113. [CrossRef]
36. Meng, Y.Y.; Tian, X.L.; Li, Z.W.; Zhou, W.; Zhou, Z.J.; Zhong, M.H. Comparison analysis on complex topological network models of urban rail transit: A case study of Shenzhen Metro in China. *Phys. A Stat. Mech. Its Appl.* **2020**, *559*, 125031. [CrossRef]
37. Chen, H.Y.; Zhang, L.M.; Ran, L.Y. Vulnerability modeling and assessment in urban transit systems considering disaster chains: A weighted complex network approach. *Int. J. Disaster Risk Reduct.* **2021**, *54*, 102033. [CrossRef]
38. Lu, Q.C.; Zhang, L.; Xu, P.C.; Cu, X.; Li, J. Modeling network vulnerability of urban rail transit under cascading failures: A coupled map lattices approach. *Reliab. Eng. Syst. Saf.* **2022**, *221*, 108320. [CrossRef]
39. Shen, Y.; Gang, R.; Bin, R. Analysis of cascading failure induced by load fluctuation and robust station capacity assignment for metros. *Transp. A Transp. Sci.* **2022**, *18*, 1401–1419. [CrossRef]
40. Zhao, Y.; Zhu, Z.; Zhang, Y.; Yang, Y.; Guo, Y.; Zhou, W. Unveiling the evolution of urban rail transit network: Considering ridership attributes. *Transp. Lett.* **2024**, *17*, 310–321. [CrossRef]
41. Zhang, Y.; Shuai, B.; Zhou, J.; Yin, D.; Huang, W. Should the multi-layer transportation network structure be reduced? *Transp. Lett.* **2024**, *17*, 1079–1090. [CrossRef]
42. Xin, Z.; Niu, F. Structure and robustness of China's railway transport network. *Transp. Lett.* **2023**, *15*, 375–385. [CrossRef]
43. Hong, J.; Tamakloe, R.; Lee, S.; Park, D. Exploring the topological characteristics of complex public transportation networks: Focus on variations in both single and integrated systems in the Seoul metropolitan area. *Sustainability* **2019**, *19*, 5404. [CrossRef]
44. Shanmukhappa, T.; Ho, I.W.; Tse, C.; Leung, K. Recent development in public transport network analysis from the complex network perspective. *IEEE Circuits Syst. Mag.* **2019**, *19*, 39–65. [CrossRef]
45. Yu, C.C.; Dong, W.T.; Lin, H.C.; Lu, Y.G.; Wan, C.; Yin, Y.; Qin, Z.T.; Yang, C.; Yuan, Q. Multi-layer regional railway network and equitable economic development of megaregions. *npj Sustain. Mobil. Transp.* **2025**, *2*, 3. [CrossRef]
46. Kim, J.; Schmöcker, J.D.; Yu, J.W.; Choi, J.Y. Service quality evaluation for urban rail transfer facilities with Rasch analysis. *Travel Behav. Soc.* **2018**, *13*, 26–35. [CrossRef]
47. Wu, Z.; Ji, X.; Zhou, X.; Tong, S. Research on environmental suitability evaluation of the transfer spaces in urban subway stations. *Buildings* **2022**, *12*, 2209. [CrossRef]
48. Sadhukhan, S.; Banerjee, U.K.; Maitra, B. Preference heterogeneity towards the importance of transfer facility attributes at metro stations in Kolkata. *Res. Transp. Bus. Manag.* **2018**, *12*, 72–83. [CrossRef]
49. Melody, K.S.; John, P.; Mona, K.S. Evaluating efficiency of passenger railway stations: A DEA approach. *Res. Transp. Bus. Manag.* **2016**, *20*, 33–38. [CrossRef]
50. Zhou, Z.Y.; Yang, M.; Cheng, L.; Yuan, Y.L.; Gan, Z.X. Do passengers feel convenient when they transfer at the transportation hub? *Travel Behav. Soc.* **2022**, *29*, 65–77. [CrossRef]
51. Lee, E.H.; Lee, H.; Kho, S.Y. Evaluation of transfer efficiency between bus and subway based on data envelopment analysis using smart card data. *KSCE J. Civ. Eng.* **2019**, *23*, 788–799. [CrossRef]
52. Schettini, T.; Jabali, O.; Malucelli, F. Demand-driven timetabling for a metro corridor using a short-turning acceleration strategy. *Transp. Sci.* **2022**, *56*, 919–937. [CrossRef]
53. Zhang, Q.; Li, X.; Yan, T.; Lu, L.L.; Shi, Y. Last train timetabling optimization for minimizing passenger transfer failures in urban rail transit networks: A time period based approach. *Phys. A Stat. Mech. Its Appl.* **2022**, *605*, 128071. [CrossRef]
54. He, D.; Yang, Y.J.; Chen, Y.; Deng, J.X.; Shan, S.; Liu, J.R.; Li, X.W. An integrated optimization model of metro energy consumption based on regenerative energy and passenger transfer. *Appl. Energy* **2020**, *264*, 114770. [CrossRef]
55. Yan, L.; Si-Rui, N.; Yue, G.; Cai-Hua, Z.; Duo, L. Detection and analysis of transfer time in urban rail transit system using WIFI data. *Transp. Lett.* **2022**, *15*, 634–644. [CrossRef]
56. Yan, D.M.; Guo, J.H.; Liu, Z.; Huang, W. A novel hybrid evaluation method for transfer efficiency assessment between rail transit and public bicycles. *Promet-Traffic Transp.* **2020**, *2*, 279–282. [CrossRef]

57. Cheng, Y.; Ye, X.; Fujiyama, T. How does interchange affect passengers' route choices in urban rail transit?—A case study of the Shanghai Metro. *Transp. Lett.* **2021**, *14*, 416–426. [CrossRef]
58. Chen, Z.Y.; ZHuang, F.; Yang, L.L.; Zheng, J. Evaluation of transfer efficiency between subway and bus based on the interval number ranking method by employing probability reliability: Taking Ningbo for example. *Discret. Dyn. Nat. Soc.* **2021**, *2021*, 9125605. [CrossRef]
59. Gu, W.; Zhang, K.; Zhou, Z.; Jin, M.; Zhou, Y.; Liu, X.; Spanos, C.J.; Shen, Z.J.M.; Lin, W.H.; Zhang, L. Measuring fine-grained metro interchange time via smartphones. *Transp. Res. Part C Emerg. Technol.* **2017**, *81*, 153–171. [CrossRef]
60. Sun, X.Z.; Xu, C.; Gao, Y.N. How urban form shapes bike-metro integration: A multidimensional typology of usage patterns and accessibility inequities. *Travel. Behav. Soc.* **2025**, *41*, 101080. [CrossRef]
61. Du, M.Y.; Li, X.F.; Cheng, L.; Lu, W.K.; Li, W.X. Order matching optimization of the ridesplitting service: A scenario with midway stops. *Transp. Res. Part E Logist. Transp. Rev.* **2025**, *194*, 103936. [CrossRef]
62. Jaber, A.; Baker, L.A.; Csonka, B. The Influence of Public Transportation Stops on Bike-Sharing Destination Trips: Spatial Analysis of Budapest City. *Future Transp.* **2022**, *2*, 688–697. [CrossRef]
63. Qian, X.; Jaller, M.; Circella, G. Exploring the potential role of bikeshare to complement public transit: The case of San Francisco amid the coronavirus crisis. *Cities* **2023**, *137*, 104290. [CrossRef]
64. Kim, M.; Cho, G.-H. Examining the causal relationship between bike-share and public transit in response to the COVID-19 pandemic. *Cities* **2022**, *131*, 104024. [CrossRef]
65. Solecka, K.; Hoy, K.N.; Deryło, A. Assessment of transport interchanges for the needs of people with reduced mobility. *Travel. Behav. Soc.* **2020**, *21*, 48–56. [CrossRef]
66. Lachapelle, U.; Boisjoly, G. Breaking down public transit travel time for more accurate transport equity policies: A trip component approach. *Transp. Res. Part A Policy Pract.* **2023**, *175*, 103756. [CrossRef]
67. Han, Y.; Ku, J.; Kim, Y.; Hwang, J. Analyzing accessibility of subway stations for the transport-vulnerable population segments in Seoul: Case of bus to subway transfer. *Case Stud. Transp. Policy* **2022**, *10*, 166–174. [CrossRef]
68. Kujala, R.; Weckström, C.; Mladenović, M.N.; Saramäki, J. Travel times and transfers in public transport: Comprehensive accessibility analysis based on Pareto-optimal journeys. *Comput. Environ. Urban Syst.* **2018**, *114*, 94–109. [CrossRef]
69. Zhu, J.; Rui, X. Spatiotemporal Dynamics and Multi-Scale Equity Evaluation of Urban Rail Accessibility: Evidence from Hangzhou. *ISPRS Int. J. Geo-Inf.* **2025**, *14*, 361. [CrossRef]
70. Sun, H.N.; Li, K.P.; Ma, Z.; Xu, Y.X.; Liang, Y. Passenger Travel Behavior in Urban Rail Transit Based on the Networked Model. *Commun. Theor. Phys.* **2025**, *77*, 125001. [CrossRef]
71. Zhu, Z.J.; Zeng, J.; Gong, X.L.; He, Y.D.; Qiu, S.C. Analyzing Influencing Factors of Transfer Passenger Flow of Urban Rail Transit: A New Approach Based on Nested Logit Model Considering Transfer Choices. *Int. J. Environ. Res. Public Health* **2021**, *18*, 8462. [CrossRef]
72. Mao, C.Y.; Xu, W.J.; Huang, Y.W.; Zhang, X.T.; Zheng, N.; Zhang, X.H. Investigation of Passengers' Perceived Transfer Distance in Urban Rail Transit Stations Using XGBoost and SHAP. *Sustainability* **2023**, *15*, 7744. [CrossRef]
73. Nigam, A.; Srivastava, S. Hybrid deep learning models for traffic stream variables prediction during rainfall. *Multimodal Transp.* **2023**, *2*, 100052. [CrossRef]
74. Huang, F.; Wang, Z.; Jiang, L.; Hua, F. Machine learning-based intelligent parameterization of source functions in numerical wave model. *Ocean Modell.* **2025**, *198*, 102602. [CrossRef]
75. Peng, Y.; Lei, K.; Yang, X.; Peng, J. Improved chaotic quantum-behaved particle swarm optimization algorithm for fuzzy neural network and its application. *Math. Probl. Eng.* **2020**, *2020*, 9464593. [CrossRef]
76. Ribeiro, M.; Singh, S.; Guestrin, C. Why should I trust you?: Explaining the predictions of any classifier. In Proceedings of the 22nd ACM SIGKDD International Conference on Knowledge Discovery and Data Mining, San Francisco, CA, USA, 13–17 August 2016; pp. 1135–1144. [CrossRef]
77. Štrumbelj, E.; Kononenko, I. Explaining prediction models and individual predictions with feature contributions. *Knowl. Inf. Syst.* **2014**, *41*, 647–665. [CrossRef]

Disclaimer/Publisher's Note: The statements, opinions and data contained in all publications are solely those of the individual author(s) and contributor(s) and not of MDPI and/or the editor(s). MDPI and/or the editor(s) disclaim responsibility for any injury to people or property resulting from any ideas, methods, instructions or products referred to in the content.